

# The algorithm of fast image stitching based on multi-feature extraction

Cite as: AIP Conference Proceedings **1967**, 040037 (2018); <https://doi.org/10.1063/1.5039111>  
Published Online: 23 May 2018

Chunde Yang, Ge Wu, and Jing Shi



View Online



Export Citation

## ARTICLES YOU MAY BE INTERESTED IN

**THTM: A template matching algorithm based on HOG descriptor and two-stage matching**  
AIP Conference Proceedings **1955**, 040131 (2018); <https://doi.org/10.1063/1.5033795>

## Lock-in Amplifiers up to 600 MHz

starting at  
\$6,210



 Zurich  
Instruments

Watch the Video



# The Algorithm of Fast Image Stitching Based on Multi-feature Extraction

Chunde Yang<sup>1</sup>, Ge Wu<sup>1</sup>, Jing Shi<sup>2</sup>

<sup>1</sup> College of Computer Science & Technology, Chongqing University of Posts & Telecommunications, Chongqing 400065, China;

<sup>2</sup> College of Computer Science, Chongqing University, Chongqing 400044, China

**Abstract.** This paper proposed an improved image registration method combining Hu-based invariant moment contour information and feature points detection, aiming to solve the problems in traditional image stitching algorithm, such as time-consuming feature points extraction process, redundant invalid information overload and inefficiency. First, use the neighborhood of pixels to extract the contour information, employing the Hu invariant moment as similarity measure to extract SIFT feature points in those similar regions. Then replace the Euclidean distance with Hellinger kernel function to improve the initial matching efficiency and get less mismatching points, further, estimate affine transformation matrix between the images. Finally, local color mapping method is adopted to solve uneven exposure, using the improved multiresolution fusion algorithm to fuse the mosaic images and realize seamless stitching. Experimental results confirm high accuracy and efficiency of method proposed in this paper.

**Key words:** SIFT feature; Outline structure; Image mosaic; Uniform treatment of exposure; Multi resolution fusion.

## INTRODUCTION

Image stitching registers and combines multiple photographic images with overlapping fields of view to produce a seamless panorama or high-resolution image after resampling. As a very promising technology in application, it is both theoretically and practically significant in such fields as virtual reality, remote sensing image processing and medical image analysis.

At present, mainstream techniques for stitching include image registration [1-2] and image fusion [3]. Among them, image registration decides the quality and timeliness of image stitching to a large degree, but it may be based on regional features [4] or feature points. The image stitching technique based on regional features allows image registration by calculating the similarities between image blocks, so it is characterized by fast processing and high efficiency as well as poor scaling and rotary robustness. Differently, the image stitching technique based on feature points elaborates the relationship between pixels to find out the correlation between images and identify where they match. However, this technique consumes much time and memory, so it is very difficult to satisfy the real-time needs.

Considering the shortcomings of the above techniques, this paper puts forward an image registration method that combines contour structure information and feature points, utilizes the contour structure information of Hu-based invariant moments [5] to find out the overlapping fields between two images, and further extracts features using the scale invariant feature transform (SIFT) algorithm in the overlapping fields. Then Hellinger kernel function is employed to improve the accuracy of initial matching. At the stage of image fusion, brightness equalization and color mapping of images are carried out before the improved wavelet transform multi-resolution fusion technique is used. Eventually, seamless panorama with satisfying effect of fusion is obtained.

## TRADITIONAL IMAGE REGISTRATION MODEL

### Extraction of SIF Feature Points

The SIFT algorithm [6] is often used to extract features as it can maintain the immutability for rotation, scaling, and brightness variability, and keep stable to some extent during the change of perspective or the existence of noise. The extraction is performed as follows: use the continuously changing Gaussian kernel function to convolute images in different scale spaces; detect key points in the obtained scale spaces of images, and mark the candidate feature points if such points are extreme points; use three-dimensional quadratic function to accurately locate key points, and assign direction to each key point, so as to guarantee the rotational immutability of SIFT features.

### Matching and Accurate Registration of Feature Points

After extracting the feature points of images, image registration will be carried out in the following process: establish the KD-tree for reference image and target image respectively, use KNN algorithm for matching, and calculate the Euclidean distance to obtain the results of initial matching; employ the RANSAC algorithm [7] to conduct accurate matching for feature points generated from rough matching. Constantly obtain the desired matching pairs through iterative estimation from the set of feature points generated from initial matching, and then perform the affine transformation [8].

## IMPROVED IMAGE REGISTRATION MODEL

Traditional registration model is time-consuming and faces redundant invalid feature point overload as it addresses images globally, but these problems can be effectively resolved with the method proposed in this paper. At first, the overlapping fields of images to be stitched are obtained using contour features, and SIFT algorithm is employed to extract features in the overlapping fields. In this way, the accuracy of image registration can be improved in a shortened period of feature extraction by combining contour features and SIFT feature points.

### Accelerated Processing of Contour Features

Binarization with adaptive threshold is first performed for the original images, and rapid contour extraction is conducted using the model for neighborhood of pixels. After that, multiple equidistance iterative calculations are performed using matrix-based similarity measure to quickly estimate the similar regions between the images to be stitched.

The specific steps of the proposed contour field calculation are as follows:

(i) Input two images to be stitched, i.e.  $L$  and  $R$  (make  $L$  stand for left image and  $R$  right image). Perform wave filtering to eliminate noise disturbance, and then perform the binarization with adaptive threshold to obtain the corresponding binary images  $L_{binary}$  and  $R_{binary}$ ;

(ii) Carry out hole filling for images  $L_{binary}$  and  $R_{binary}$ , and quickly extract the contour structure information to further obtain the images  $L_{binary}^*$  and  $R_{binary}^*$ ;

(iii) Invert the colors of binary images  $L_{binary}^*$  and  $R_{binary}^*$  (i.e. 0 stands for black pixels and 1 white pixels). When the pixel value is 1, identify whether there is 0 in its neighborhood. If yes, the pixel value remains unchanged, or it should be inverted. After this processing, the images with contour structure information are obtained, i.e.  $L_{contour}$  and  $R_{contour}$ . The images in the above steps are obtained as presented in Fig. 1.

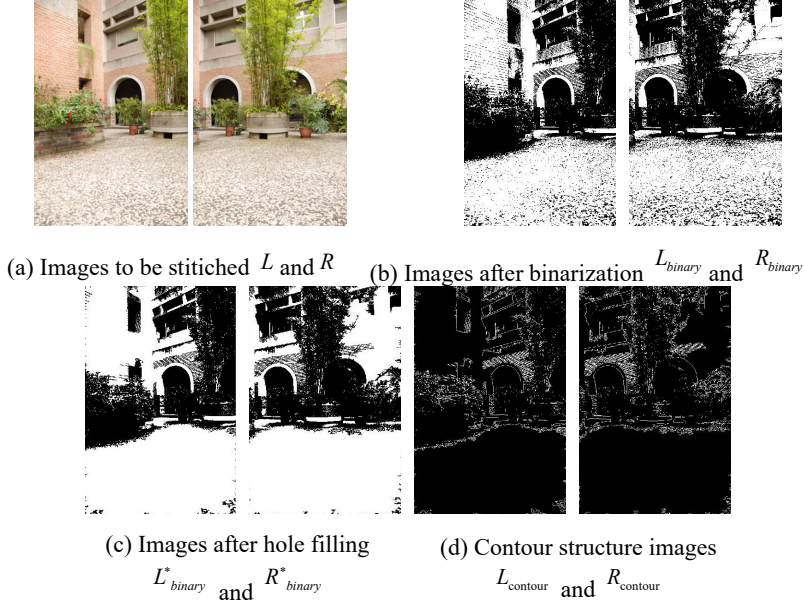


FIG. 1 Steps of contour information extraction

### Similarity Measurement Based on Hu Invariant Moment Features

Hu invariant moment, as a regional feature of image, can greatly describe the shape and contour of object, and remain unchanged with regard to such features as rotation, translation and scale. Therefore, this paper takes Hu invariant moment eigenvector for the similarity measurement of images. The specific steps of calculation are as follows:

(i) Take a region  $L_{contour}^i$  with the width  $20 \times i (1 \leq i < N)$  and the height  $H$  from right to left on the binary image  $L_{contour}$  at the step of  $N (N = W / 20)$ , and a region  $R_{contour}^i$  with the width  $20 \times i (1 \leq i < N)$  and the height  $H$  from left to right on the binary image  $R_{contour}$ .

(ii) Calculate the center of mass  $(x^*, y^*)$  of contour for different regions in the above  $L_{contour}$  and  $R_{contour}$  with the formula (1):

$$\begin{cases} x^* = \frac{\sum_{y=1}^H \sum_{x=1}^{20 \times i} x I(x, y)}{\sum_{y=1}^H \sum_{x=1}^{20 \times i} I(x, y)} \\ y^* = \frac{\sum_{y=1}^H \sum_{x=1}^{20 \times i} y I(x, y)}{\sum_{y=1}^H \sum_{x=1}^{20 \times i} I(x, y)} \end{cases} \quad 1 \leq i < N \quad (1)$$

(iii) Normalize the centre distance of  $p + q$  order between  $L_{contour}$  and  $R_{contour}$  as follows:

$$\begin{cases} \mu_{pq} = \sum_{y=1}^H \sum_{x=1}^{20 \times i} (x - x^*)^p (y - y^*)^q I(x, y) \\ \eta_{pq} = \mu_{pq} / (\mu_{00}^\rho) \end{cases} \quad , p, q \in \{0, 1, 2\} \quad (2)$$

In which, when  $p+q=2$ , the parameter is  $\rho = 2$ . When  $p+q=3$ , the parameter is  $\rho = 2.5$ . Hence, the contour similarity detection is satisfying.

(iv) Reduce time complexity by simplifying 7 Hu invariant moments into 4-dimensional eigenvectors. Construct two-order invariant moments  $M_1$  and  $M_2$  of  $L_{\text{contour}}$  and  $R_{\text{contour}}$  to ensure scale invariant contour feature;

$$\begin{cases} M_1 = \eta_{20} + \eta_{02} \\ M_2 = (\eta_{20} - \eta_{02})^2 + 4\eta_{11}^2 \end{cases} \quad (3)$$

(v) Construct three-order invariant moments  $M_3$  and  $M_4$  of  $L_{\text{contour}}$  and  $R_{\text{contour}}$  to ensure rotation invariant contour feature;

$$\begin{cases} M_3 = (\eta_{30} - 3\eta_{12})^2 + (3\eta_{21} - \eta_{03})^2 \\ M_4 = (\eta_{30} + 3\eta_{12})^2 + (\eta_{21} + \eta_{03})^2 \end{cases} \quad (4)$$

(vi) Calculate the distance of moment vector between two images using invariant moments  $M = \{M_1, M_2, M_3, M_4\}$ . The shorter distance, the higher contour similarity. Calculate the  $M_{L_{\text{contour}}}$  and  $M_{R_{\text{contour}}}$  of image contour in the regions obtained in (i).

(vii) Sum up the similarity measures  $r_i$  of  $L_{\text{contour}}^i$  and  $R_{\text{contour}}^i$  from each calculation. The maximum value  $r_{\max} = \text{MAX}\{r_i\}$  indicates the similarity between the corresponding regions of  $L$  and  $R$ . The similar regions of  $L$  and  $R$  are marked with overlay (coordinates of starting point  $(x, y)$ , region width and region height):

$$\begin{cases} L_{\text{overlay}} = (W - 20 \times i, 0, 20 \times i, H) \\ R_{\text{overlay}} = (0, 0, 20 \times i, H) \end{cases} \quad (5)$$

In which,  $1 \leq i < N$  and  $i$  are corresponding to  $r_i = r_{\max}$ . The summed information is presented in Fig. 2.

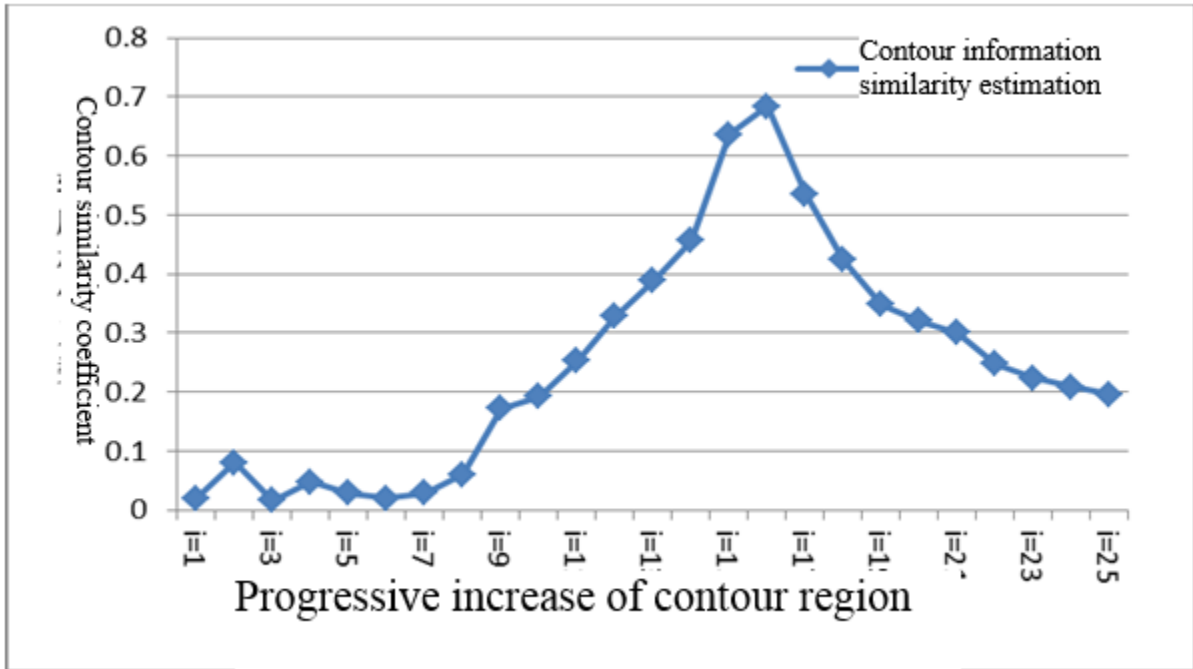
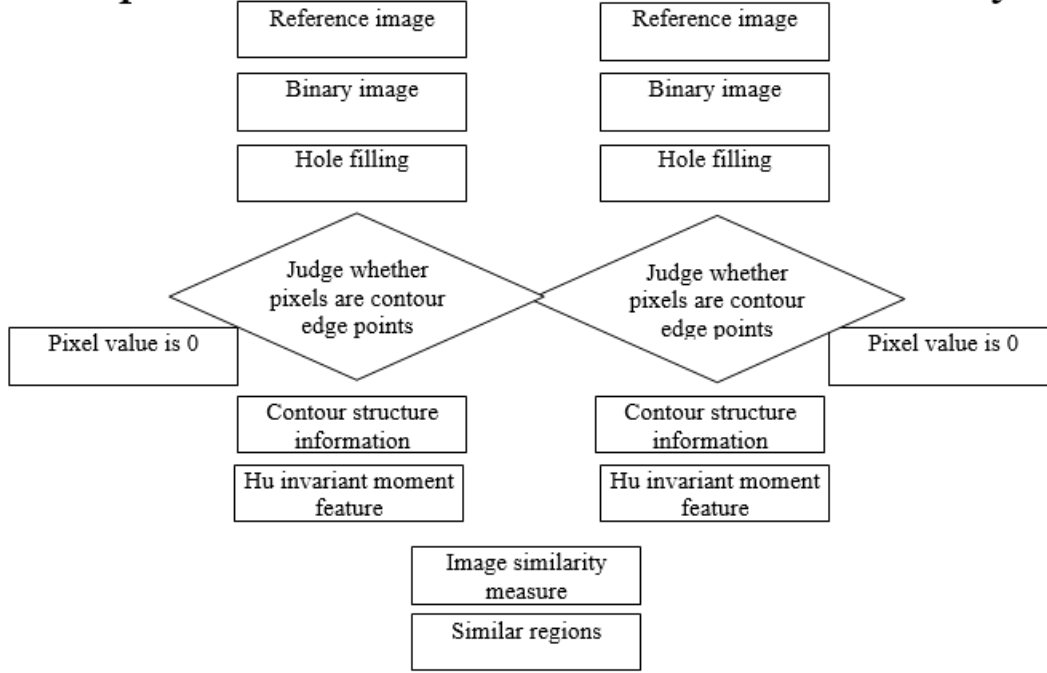


FIG. 2 Progressive increase distribution of contour similarity between two images

The process of contour extraction and similarity measurement is presented in Fig. 3.



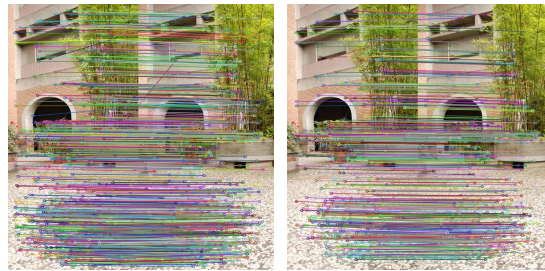
**FIG. 3** Process flow of contour extraction and similarity measurement

### Improvement of SIFT Feature Matching

This paper employs the Hellinger kernel function to measure SIFT eigenvectors, which may improve the performance of feature description. Traditional SIFT utilizes Euclidean distance for feature calculation. As revealed in experimental results, Hellinger kernel function is timelier than Euclidean distance. The vector sets of SIFT feature points in the overlapping regions of two images are  $X$  and  $Y$ , and Hellinger kernel function is employed to normalize  $X$  and  $Y$  (i.e.  $\sum_{i=1}^{128} X_i = 1, x_i \geq 0$ ). The expression for the calculation of 128-dimensional feature distance based on SIFT algorithm is as follows:

$$H(X, Y) = \sum_{i=1}^{128} \sqrt{X_i Y_i} \quad (6)$$

After initial matching of two images with Hellinger kernel function, RANSAC algorithm is utilized to eliminate mismatching points and estimate the affine transform matrix  $H$ . The matching results are shown in Fig. 4.



(a) Initial matching with Hellinger kernel

(b) Accurate matching with RANSAC

**FIG. 4** matching results

## MULTI-RESOLUTION IMAGE FUSION

Due to their difference in exposure and lighting [9-10], two images to be stitched have different levels of brightness and contrast. The difference should be lowered prior to image fusion.

### Brightness Equalization and Local Color Mapping

This paper conducts the linear transformation mapping of standard deviation for reference image through brightness equalization and local color mapping. At first, color spatial transformation is performed for source image and image to be stitched, and the means and standard deviations of three channels L, A and B for such images are calculated as follows:

$$(\bar{L}_i, \bar{a}_i, \bar{b}_i, \sigma_i^l, \sigma_i^a, \sigma_i^b), (\bar{L}_j, \bar{a}_j, \bar{b}_j, \sigma_j^l, \sigma_j^a, \sigma_j^b).$$

Formula (7) is used for local color mapping:

$$\begin{cases} L^* = (L_i - \bar{L}_i) * \frac{\sigma_j^l}{\sigma_i^l} + \bar{L}_j \\ a^* = (a_i - \bar{a}_i) * \frac{\sigma_j^a}{\sigma_i^a} + \bar{a}_j \\ b^* = (b_i - \bar{b}_i) * \frac{\sigma_j^b}{\sigma_i^b} + \bar{b}_j \end{cases} \quad (7)$$

$L^*$ ,  $a^*$  and  $b^*$  are transformed into RGB color space to obtain the image to be fused.

### Multi-resolution Image Fusion Based on Wavelet Transform of Contour Region

In this paper, the improved wavelet transform multi-resolution fusion method is employed for image fusion. On the basis of numerous experiments, the empirical threshold  $\xi$  ( $\xi=30$ ) for the limited scope of fusion is obtained. Within this scope, image fusion guarantees efficiency and shorter period of fusion. By limiting with the left and right boundaries of the overlapping region, the rectangle  $U$  has the left boundary  $x_l - \xi$  and the right boundary  $x_r + \xi$ .

The improved wavelet transform fusion is conducted to eliminate the stitching seams in the following steps:

(i) Perform the wavelet pyramid decomposition of images for the generated regions to be fused, i.e.  $U_L$  and  $U_R$ .

(ii) Fuse different components of frequency at each decomposition level using different fusion operators to obtain fused wavelet pyramid. Employ the weighted average method in the low-frequency region, and the maximum absolute method in the high-frequency region.

(iii) Conduct inverse wavelet transformation for the wavelet pyramid from fusion to obtain the restructured image, i.e. fused image.

The whole fusion process can be described with Formula (8):

$$U^* = W^{-1}[F(W\{U_i\})] \quad (8)$$

In which,  $U_i$  represents the to-be-fused region of the  $i$  th image.  $W$  and  $F$  are wavelet transform operator and fusion operator.

The experimental results of improved wavelet transform multi-resolution fusion are as shown in Fig. 5.



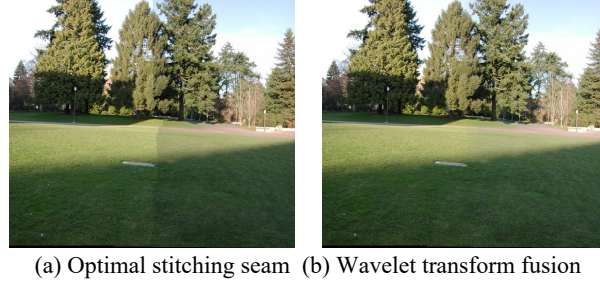


**FIG. 5** Images before and after fusion

During the sequential stitching of multiple images, errors accumulate constantly to cause skew and distortion. At last, bilinear interpolation should be carried out on the panorama to rectify its distortion.

The stitching algorithm is implemented in the process as shown in Fig. 6.

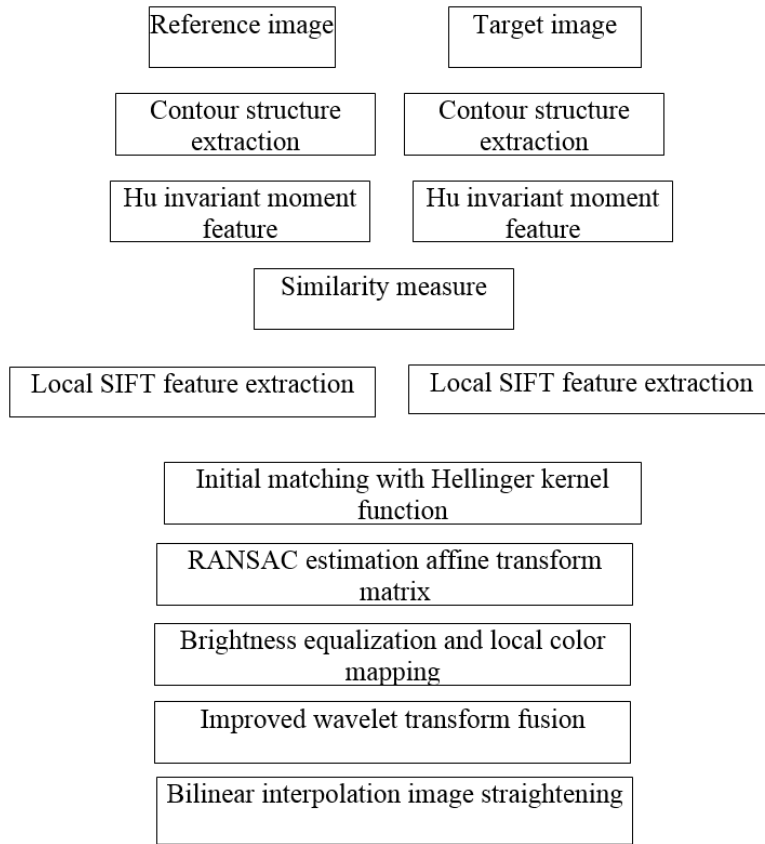
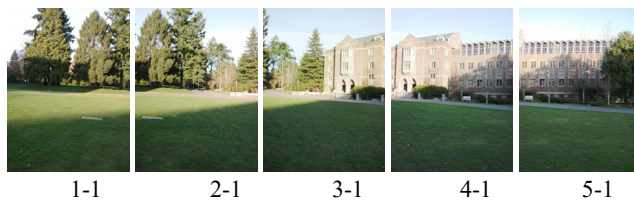


**FIG. 6** Proposed stitching algorithm process

## EXPERIMENTAL RESULTS AND ANALYSIS

In this paper, images with various scenes are stitched using the following software and hardware: CPU: Intel(R) Core(TM) i5-6200U 2.40GHz, OS: Windows 10, Library: OpenCV 2.4.9.



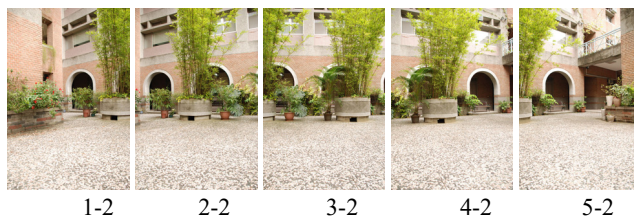


(a) 5 original sequential images with resolution  $384 \times 512$

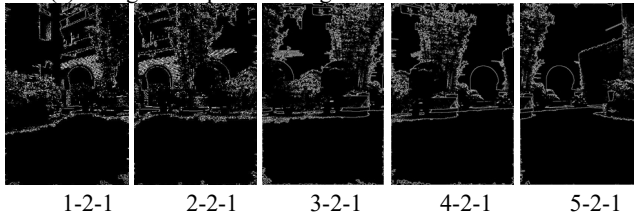


(b) Panorama of sequential scene (a) obtained with the proposed algorithm

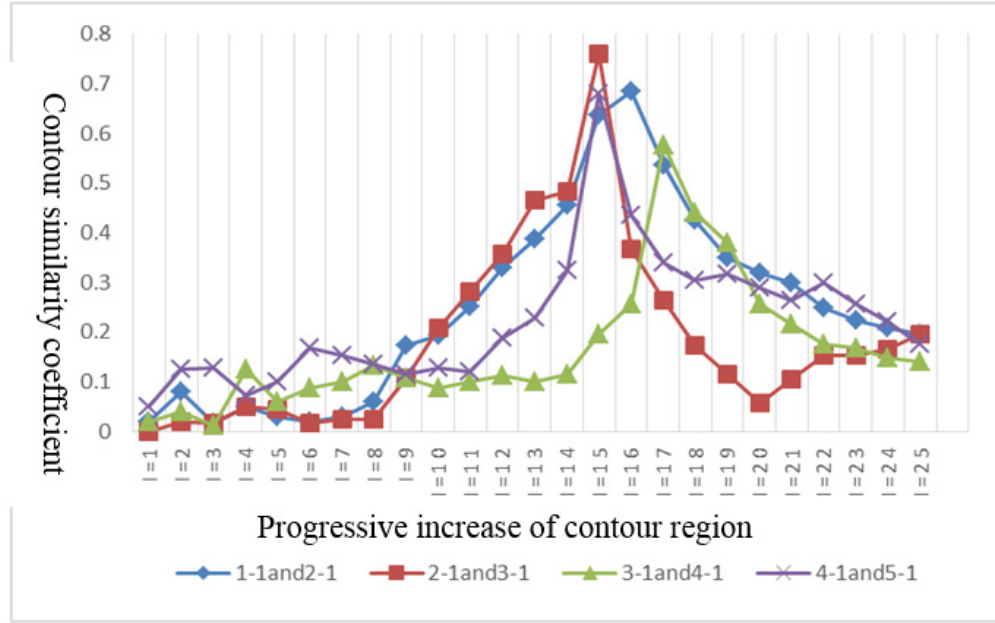
**FIG. 7** Empirical result of sequential scene (a)



(a) 5 original sequential images with resolution  $500 \times 747$



(b) 5 sequential contour information images with resolution  $500 \times 747$



(c) Progressive increase distribution of neighboring contour similarity by region for sequential image



(d) Panorama of sequential scene (b) obtained with the proposed algorithm

**FIG. 8** Empirical results of sequential image (b)

Fig. 7 (a) and (b) present the original sequential images of scene (a) and their panorama obtained with the proposed algorithm respectively. Fig. 8 (a), (b), (c) and (d) show the original sequential images of scene (b) and their contour information sequential images, regional similarity distribution between images, and panorama obtained with the proposed algorithm respectively.

**TABLE 1.** Comparison of experimental data for extracted feature points of sequential scene (a)

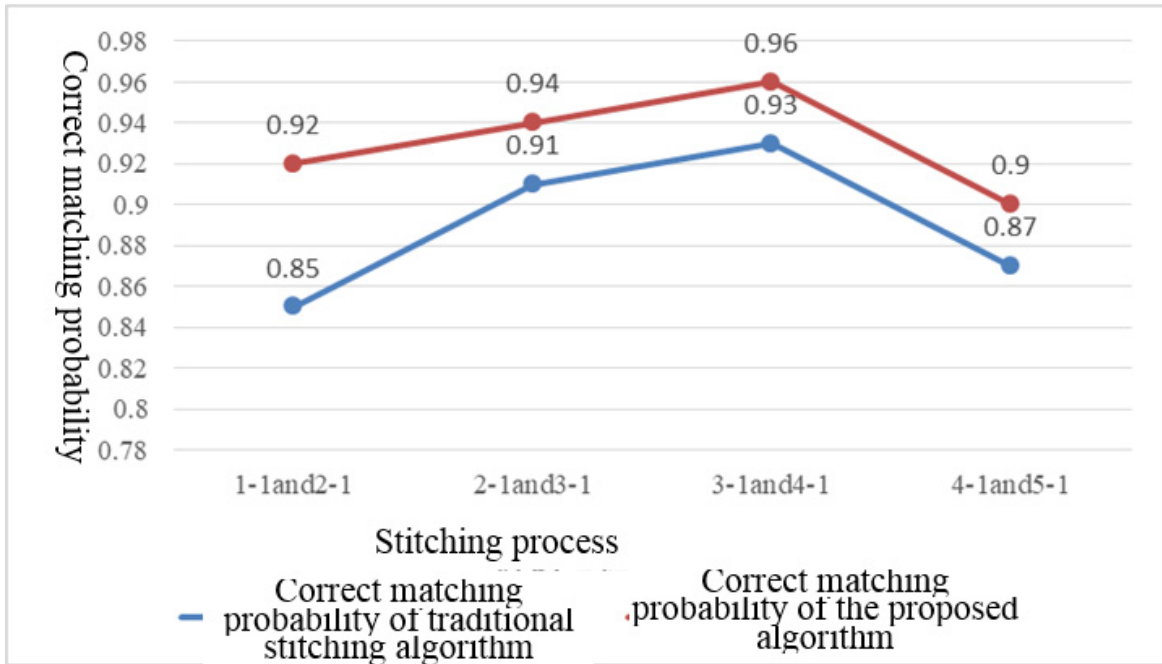
Image	Number of Feature Points		Time of Feature Point Extraction (ms)	
	SIFT	Improved	SIFT	Improved
<b>Image1-1</b> 384 × 512	1379	912	1638	1128
<b>Image2-1</b> 384 × 512	1407	970	1560	996
<b>Image3-1</b> 384 × 512	1022	782	1404	1082
<b>Image4-1</b> 384 × 512	1007	740	1358	988
<b>Image5-1</b> 384 × 512	1122	977	1436	1004

**TABLE 2.** Comparison of experimental data for extracted feature points of sequential scene (b)

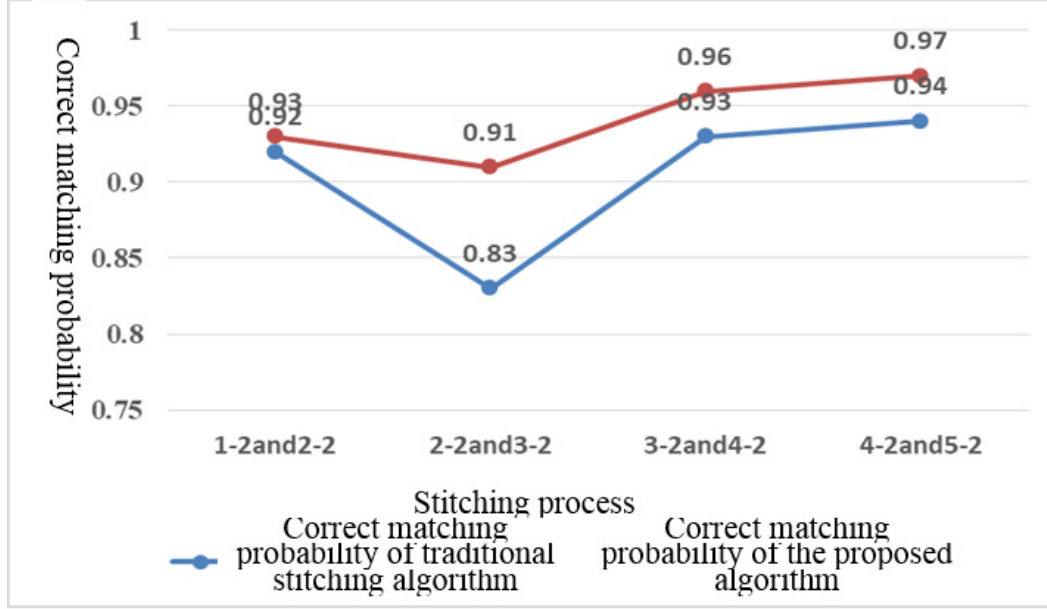
Image	Number of Feature Points		Time of Feature Point Extraction (ms)	
	SIFT	Improved	SIFT	Improved
<b>Image1-2</b> 500 × 747	5563	3552	2242	1928
<b>Image2-2</b> 500 × 747	5661	3584	2292	1982
<b>Image3-2</b> 500 × 747	5988	3791	2909	2461
<b>Image4-2</b> 500 × 747	5616	3539	2237	1851
<b>Image5-2</b> 500 × 747	5226	3240	1976	1679

The probability of correct matching between images is defined as shown in formula (9), and the experimental results are given in Fig. 9.

$$\text{Probability of correct matching} = \frac{\text{Number of matching points after removing mismatching points}}{\text{Number of points in initial matching}} \quad (9)$$



(a) Comparison of matching probabilities for sequential scene (a)



(b) Comparison of matching probabilities for sequential scene (b)

FIG. 9 Comparison of correct matching probabilities between the proposed feature matching and SIFT feature matching

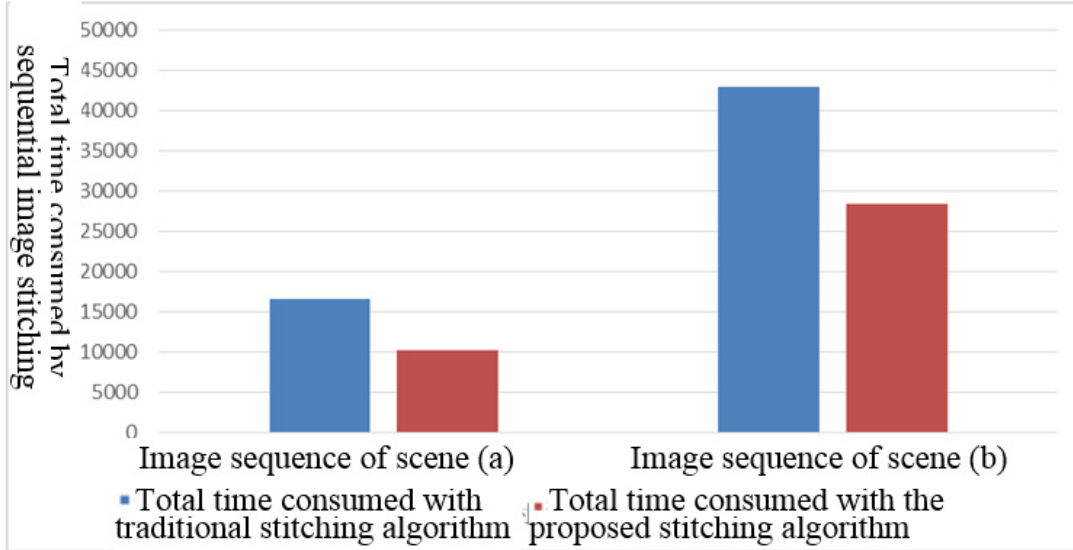


FIG. 10 Comparison of time consumed by stitching between the proposed algorithm and traditional algorithm

Obviously, the improved registration model consumes less time than using the SIFT algorithm alone. Moreover, Fig. 9 reveals that it is more possible to achieve correct matching by effectively eliminating mismatching with Hellinger kernel function and RANSAC algorithm than SIFT feature matching. Fig. 10 compares the time consumed by panorama stitching, and shows that the time consumed with the proposed algorithm is shorter than that with traditional algorithm.

## CONCLUSION

Compared with the traditional stitching algorithm, this paper proposes an image stitching algorithm with multi-feature extraction. By fully utilizing the global and local features of image, the proposed algorithm achieves better

time efficiency and less mismatching than traditional algorithm, and enhances the accuracy of feature point extraction. Meanwhile, it reduces the region of feature extraction and shortens the time of feature extraction, so as to improve the time efficiency. Considering uneven exposure and stitching seam, this paper utilizes brightness equalization and improved wavelet transform multi-resolution fusion to eliminate stitching seam. As revealed in the results of simulation experiment, the proposed algorithm improves stitching efficiency and realizes seamless image stitching.

## ACKNOWLEDGEMENTS

This work was supported by Chongqing Science & Technology commission (cstc2015jcyjBX0090)

## REFERENCES

1. LI P, WU W B, WANG Z W. Multi-source remote sensing image matching based on nonlinear scale space [J]. *Science of Surveying and Mapping*, 2015, 40(7): 41-44.
2. CHEN Yue, ZHAO Yan, WANG Shi-gang. Fast image stitching method based on SIFT with adaptive local image feature [J]. *Chinese Optics*, 2016, 9(4): 415-422
3. Huang C M, Lin S W, Chen J H. Efficient Image Stitching of Continuous Image Sequence With Image and Seam Selections[J]. *IEEE Sensors Journal*, 2015, 15(10): 5910-5918.
4. Guo Y, Bennamoun M, Sohel F, et al. A Comprehensive Performance Evaluation of 3D Local Feature Descriptors [J]. *International Journal of Computer Vision*, 2016, 116(1):66-89.
5. Noh J S, Rhee K H. Palmprint Identification Algorithm Using Hu Invariant Moments [M]// *Fuzzy Systems and Knowledge Discovery*. Springer Berlin Heidelberg, 2005:91-94.
6. Lowe D.G. Distinctive image features from scale-invariant key-points [J]. *International Journal of Computer Vision* 2004; 60(2): 91-110.
7. Qu Z, Lin S P, Ju F R, et al. The improved algorithm of fast panorama stitching for image sequence and reducing the distortion errors [J]. *Mathematical Problems in Engineering*, DOI: 10.1155/2015/428076, 2015: 1-12.
8. XUN J Z, Yuan F, Kou Y. An Image Mosaic Method Based on the Seamline and Dynamic Datum [J]. *Bulletin of Surveying and Mapping*, 2014(9): 34-37.
9. Chang C H, Sato Y, Chuang Y Y. Shape-Preserving Half-Projective Warps for Image Stitching[C]// *IEEE Conference on Computer Vision and Pattern Recognition*. IEEE Computer Society, 2014: 3254-3261.
10. Ibrahim M T, Khan M M, Khan M M, et al. Automatic selection of color reference image for panoramic stitching [J]. *Multimedia Systems*, 2016, 22(3): 379-392.